JOURNAL OF MATERIALS SCIENCE 36 (2001) 5805–5810

Electrical conduction behaviour of cobalt substituted $BaSnO_3$

O. PARKASH*,§, D. KUMAR*, K. K. SRIVASTAV‡, R. K. DWIVEDI‡
*Department of Ceramic Engineering and ‡School of Materials Science and Technology, Institute of Technology, Banaras Hindu University, Varanasi 221 005, India
E-mail: oparkash@banaras.ernet.in

A few cobalt substituted barium stannate, $BaSn_{1-x}Co_xO_3$ compositions have been synthesized by solid state ceramic method. Seebeck coefficient α has been measured as a function of temperature. Positive values of 'α' indicate that holes are the majority charge carriers. AC conductivity, σ_{ac} has been measured in the temperature range 310–550 K and frequency range 100 Hz to 10 MHz. The contributions of the grains and grainboundaries to the total conductivity have been obtained by complex plane impedance analysis. Complex plane impedance analysis shows that conduction occurs by hopping of charge carriers among localized sites.

1. Introduction

Barium stannate $BaSnO_3$ is a perovskite oxide having cubic unit cell. It forms an important constituent of dielectric compositions used for thermally stable capacitors [1, 2]. Lanthanum doped and undoped strontium stannate have been found useful as humidity sensors [3]. $BaSnO_3$ is also used as a humidity sensor [4, 5]. It has been found that it forms solid solution with $LaCoO_3$ over a wide composition range. Compositions with $x \leq 0.50$ in the system $Ba_{1-x}La_xSn_{1-x}Co_xO_3$ are single phase solid solution [6]. This system represents a valence compensated system where simultaneous substitution of trivalent Co^{3+} on tetravalent Sn^{4+} sites and trivalent La^{3+} on divalent Ba^{2+} site is expected to lead to internal charge compensation. Compositions with $0.20 \leq x \leq 0.50$ exhibit high values of dielectric constant. The value of dielectric constant changes very little with temperature over a considerable range of temperature around room temperature. These materials may be useful for thermally stable capacitors [6]. In order to understand the role played by cobalt ions in its electrical behavior, it was considered worthwhile to prepare a few compositions doped with cobalt ions only on Sn^{4+} sites. The effect of lanthanum substitution on barium sites in $BaSnO_3$ has already been studied [7]. In this paper we are reporting the results of our investigations on the synthesis, structure and electrical properties of the compositions with $x \leq 0.10$ in the system $BaSn_{1-x}Co_xO_3$. This seems to form the first report on these materials to the best of our knowledge.

2. Experimental

Compositions with $x = 0.01$, 0.05 and 0.10 were prepared by conventional solid state ceramic route. Barium carbonate, stannic oxide and cobalt oxalate, $CoC_2O_4 \cdot 2H_2O$ all having purity 99.5% or better were used as starting materials. Stoichiometric amounts of these materials were weighed and mixed in an agate mortar and pestle using acetone for 6 hours. The dried powders were calcined in platinum crucibles at 1250°C for 6 hours. The calcined powders were ground and mixed once again. These were pressed as cylindrical pellets (dia. ~12 mm), after adding a few drops of poly vinyl alcohol as binder, using a stainless steel die in a hydraulic press. These pellets were heated slowly upto 500°C in a platinum crucible and kept at this temperature for an hour to burn the binder. Temperature was then raised to 1250°C. Samples were soaked at this temperature for 12 hours for completing the solid state reaction and for sintering. After firing, the samples were furnace cooled. A few pellets were crushed into fine powder. Powder x-ray diffraction patterns were recorded using Rigaku Powder Diffractometer with 12 kW Rotating Anode Source.

Density was measured using Archemede's principle. Percentage porosity was calculated from the x-ray density and measured bulk density. For impedance measurements, the samples were polished and both the surfaces were coated with Ag-Pd paint. The pellets were fired at 700°C for 30 minutes to cure the paint. Seebeck coefficient was measured relative to platinum by pressing the sample between two spring loaded platinum foils in an indigenously fabricated sample holder. An auxiliary heater placed around one surface of the pellet was used to get a temperature gradient of 5–10°C across the sample. The entire cell assembly was heated to various steady temperatures in the range 50–700°C. A number of observations for thermo e.m.f. were taken at different temperature gradients for a given mean

§Author to whom all correspondence should be addressed.

TABLE I Structure, lattice parameter, theoretical density, experimental density and percentage porosity for different compositions in the system $BaSn_{1-x}Co_xO_3$

Compositions x	Structure	Lattice parameter a (Å)	Theoretical density (gm/cc)	Exp. density (gm/cc)	Percent Porosity
0.01	Cubic	4.115	6.99	6.51	7
0.05	Cubic	4.121	6.92	6.37	8
0.10	Cubic	4.123	6.85	5.90	14

temperature and an average value of Seebeck coefficient 'α' was determined.

3. Results and discussion

X-ray diffraction patterns of all the three compositions with $x = 0.01$, 0.05 and 0.10 in the system $BaSn_{1-x}Co_xO_3$ are similar to that of pure $BaSnO_3$ and these compositions did not contain any line characteristic of constituent oxides. This confirms the formation of single phase solid solution in these compositions. X-ray data for these compositions could be indexed on the basis of a cubic unit cell. The lattice parameters obtained by least square fitting of the XRD data using a program 'CEL' are given in Table I. It is noted that lattice parameter increases slightly with increasing x. Bulk density and % porosity are also given in Table I. It is observed that % porosity increases with increasing x.

Plots of Seebeck coefficient, α vs temperature $T(K)$ are shown in Fig. 1. α is found to be positive for all the samples over the entire temperature range of measurements. This shows that holes are the majority charge carriers, α increases slightly with increasing temperature upto a particular temperature and then remains almost constant. Value of α decreases with increasing cobalt concentration (x).

These materials have low conductivity at room temperature. Measurement of DC conductivity in low conductivity samples poses problems due to electrode polarization. In order to avoid this problem, ac conductivity of these materials was measured as a function of frequency at different steady temperatures. Plots of log σ_{ac} vs $1000/T$ at 1, 10 and 100 kHz and log σ_{ac} vs log f at several steady temperatures for compositions $x = 0.01, 0.05$ and 0.10 are shown in Fig. 2 and Fig. 3 respectively. Behavior of the composition with $x = 0.05$ is essentially similar to $x = 0.01$. It is noted that log σ_{ac} vs log f plots of $x = 0.01$ and 0.05 show a plateau in the low frequency region. This plateau is followed by a frequency dependent region. For $x = 0.10$, two plateaus, one in the low frequency range and another in the high frequency range separated by a frequency dependent region are observed. Second plateau in the high frequency range could not be observed for $x = 0.01$ and 0.05 due to limited frequency range of measurement available. DC conductivity, σ_{dc} ($\omega \to 0$) can be obtained by extrapolating the low frequency plateau to $\omega \to 0$ at a few temperatures. Plots of log σ_{dc} vs $1000/T$ for all the samples are shown in Fig. 4. All these plots are linear showing that conductivity follows Arrhenius

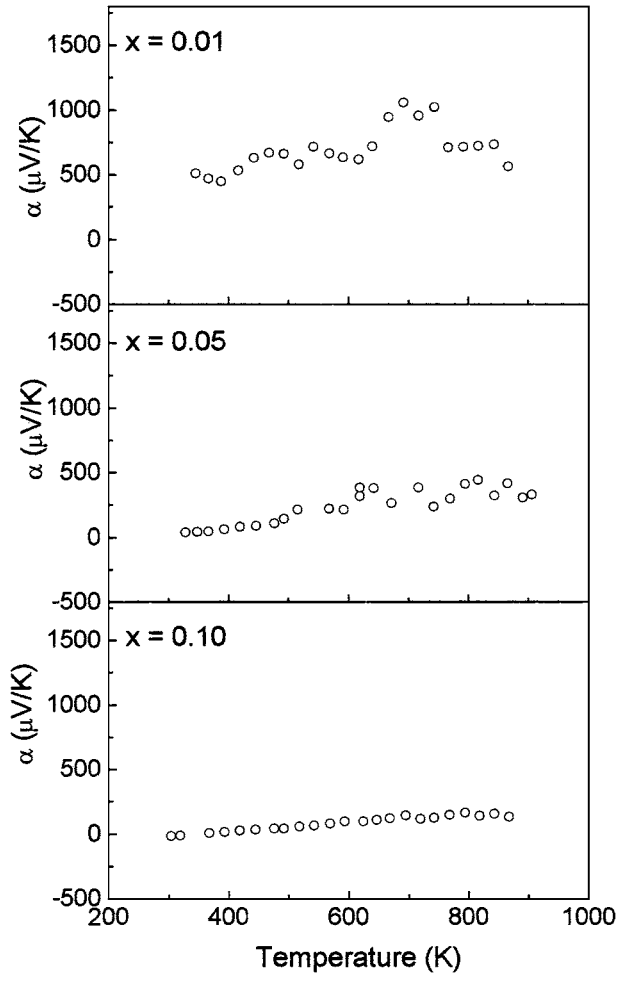

Figure 1 Variation of Seebeck coefficient 'α' with temperature for different compositions in the system $BaSn_{1-x}Co_xO_3$.

relationship.

$$\sigma_{DC} = \sigma_0 \exp\left[\frac{-E_a}{kT}\right] \quad (1)$$

where E_a is the activation energy for conduction and k is Boltzmann's constant. E_a for $x = 0.01$ is 0.38 eV while for $x = 0.05$ and 0.10 it is ~0.24 eV (Table II).

In polycrystalline ceramic materials, the defect structure and hence the electrical conduction are different for grains and grainboundaries. Plots of log σ_{ac} vs log f of these materials show frequency independent regions (plateaus) connected by frequency dependent regions. Generally one should get a plateau at low frequencies which represents the total conductivity of the sample followed by frequency dependent region in which, the relaxation of grainboundaries processes occur. This is followed by another plateau in the high frequency region, which represents the contribution of the grains (bulk) to the total conductivity. A frequency dependent

TABLE II Activation energies of conduction E_a, E_g and E_{gb} for different compositions in the system $BaSn_{1-x}Co_xO_3$

$X = 0$	E_a (eV)	E_g (eV)	E_{gb} (eV)
0.01	0.38	0.39	0.35
0.05	0.24	0.17	0.26
0.10	0.24	0.16	0.26

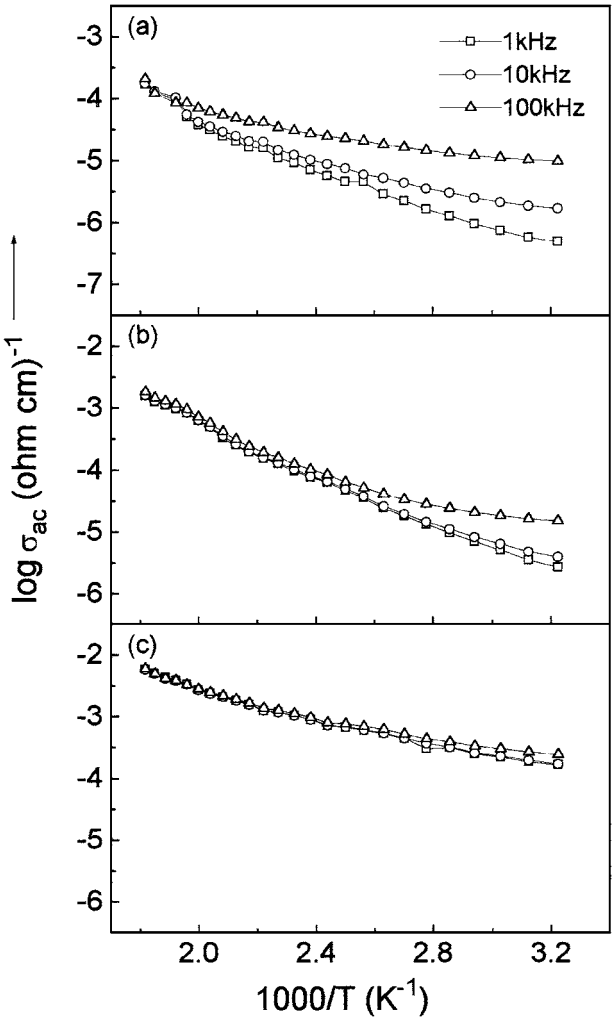

Figure 2 Variation of log σ_{ac} with 1000/T for different compositions x (a) 0.01, (b) 0.05 and (c) 0.10 in the system $BaSn_{1-x}Co_xO_3$.

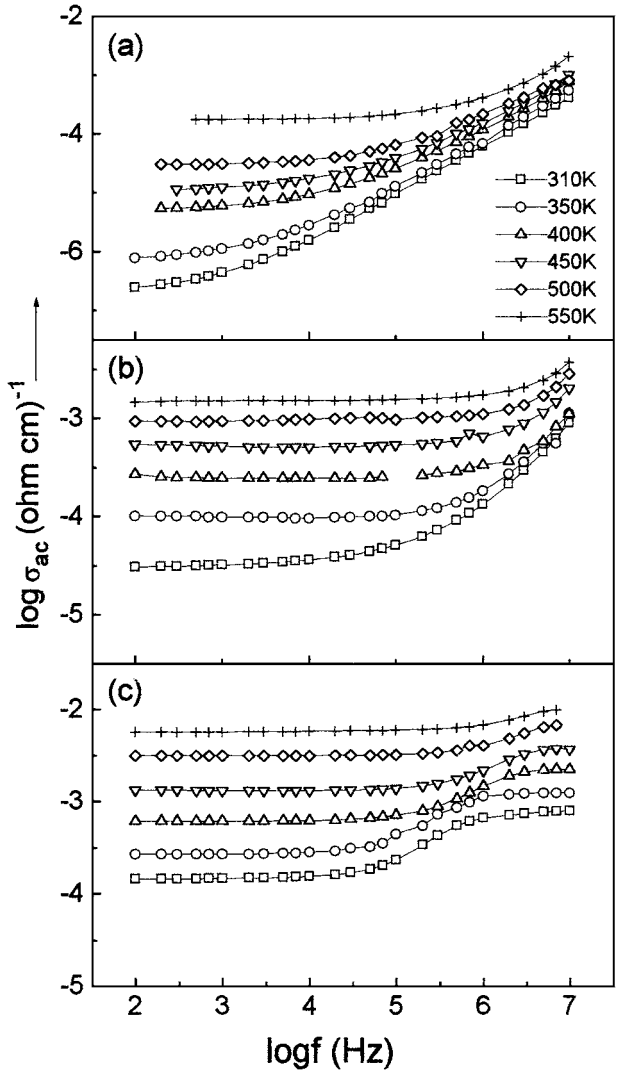

Figure 3 Variation of log σ_{ac} with log frequency for different compositions x (a) 0.01, (b) 0.05 and (c) 0.10 in the system $BaSn_{1-x}Co_xO_3$.

region occurs after the high frequency plateau, representing relaxation of bulk process. One can get the contributions of grainboundaries to the total conductivity from the difference of the conductivity values corresponding to high and low frequency plateaus.

It is noted from the Fig. 3 that the second plateau (representing the contribution of bulk or grains) could only be observed for the composition $x = 0.10$. Therefore, it is not possible to separate the contribution of grains and grainboundaries to the total conductivity for all the samples. In order to separate out the contributions of grains and grainboundaries to the total observed conductivity, complex plane impedance analysis has been used.

Complex plane impedance plots, for $x = 0.01$ at a few temperatures are shown in Fig. 5. At 310 K, the complex impedance data can be fitted to a single circular arc, passing through the origin. With increasing temperature, the data can be fitted to two and three depressed circular arcs. These plots indicate that three charge transport processes contribute to the electrical conduction in this sample. The complex impedance data for the compositions with $x = 0.05$ and 0.10 also indicate the presence of three charge transport processes in them. Complex plane impedance plots for all the three compositions at 500 K are shown in Fig. 6.

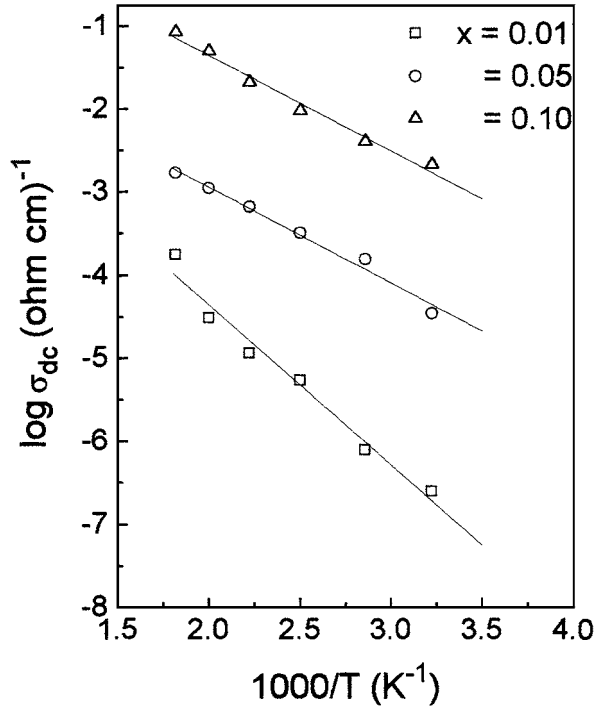

Figure 4 Variation of log σ_{dc} with 1000/T for different compositions in the $BaSn_{1-x}Co_xO_3$ system.

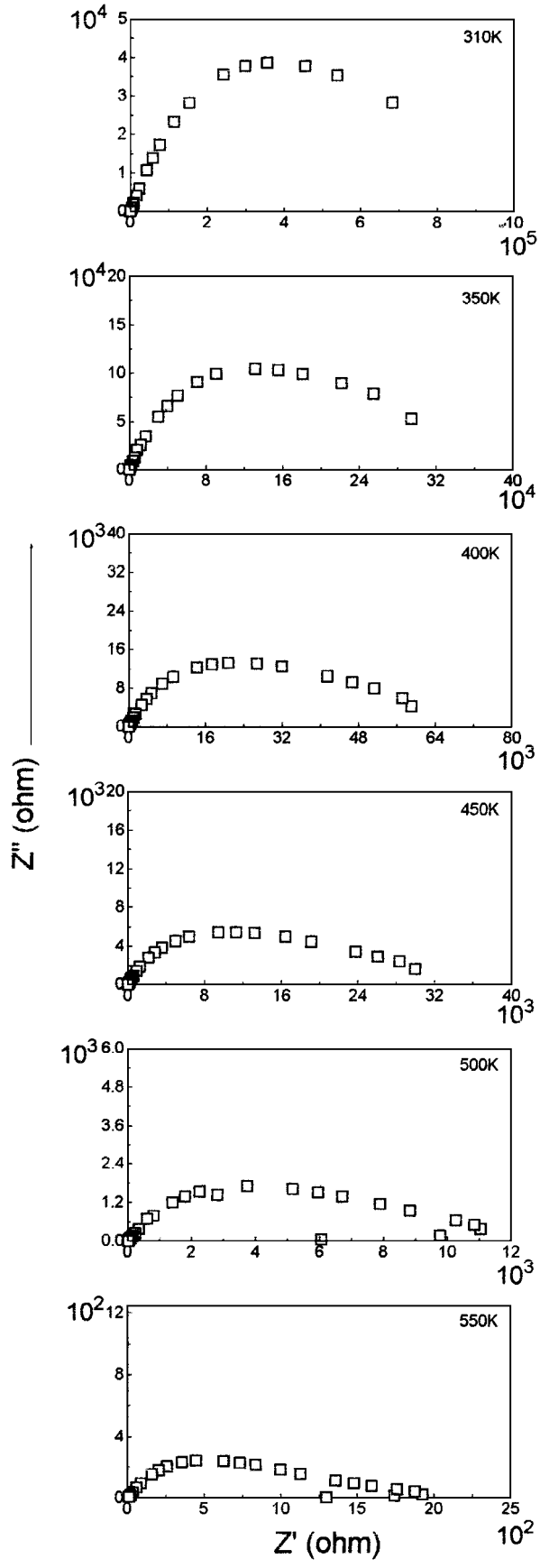

Figure 5 Complex plane impedance (Z'' vs Z') plots at a few steady temperatures for composition with $x = 0.01$ in the system $BaSn_{1-x}Co_xO_3$.

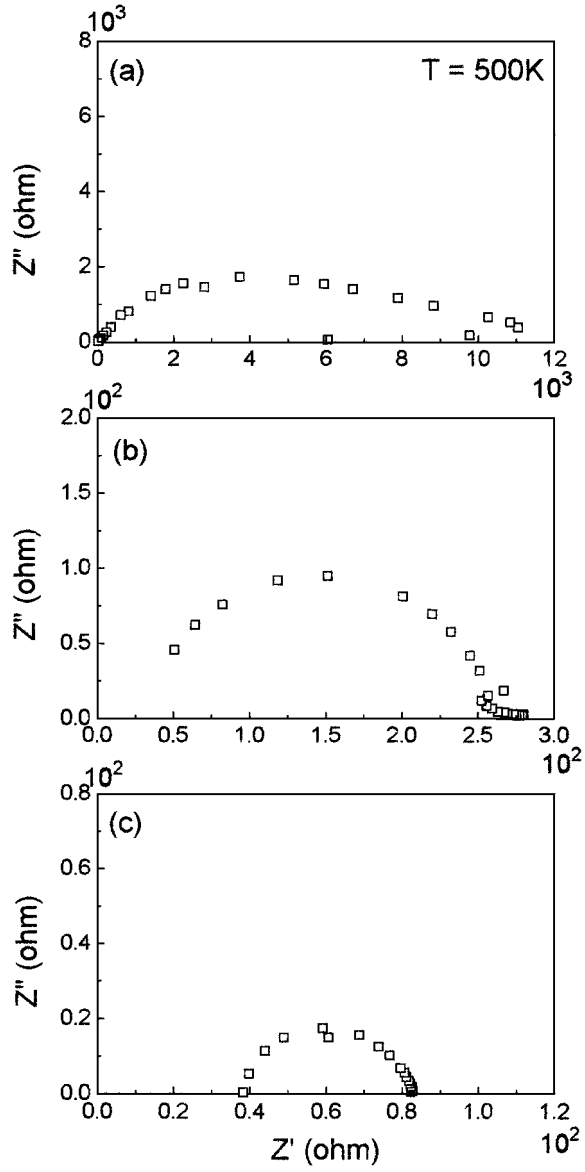

Figure 6 Typical complex plane impedance (Z'' vs Z') plots for different compositions x (a) 0.01, (b) 0.05 and (c) 0.10 in the system $BaSn_{1-x}Co_xO_3$ at 500 K.

In impedance analysis, the electrical response of a polycrystalline material is represented by an equivalent circuit. The resistance and polarization contribution of the grains, grainboundaries and sample electrode interface are usually represented by three parallel combinations of resistance R and capacitance C connected in series. If the time constant τ ($= RC$) of these circuit elements (which represent relaxation times of the electrical processes in the grains, grainboundaries and sample electrode interface) are well separated, then the complex plane impedance plots (Z'' vs Z') show three distinct semicircular arcs. If relaxation times are close to one another, then overlapping arcs are seen. If there is a distribution of relaxation times for some process, then a depressed circular arc for that process is obtained [8, 9]. Generally the arc in the highest frequency range passing through the origin is attributed to the contribution from the bulk (grains). The arc in the intermediate frequency range is attributed to the contribution from the grainboundaries and the arc in the lowest frequency range represents the contribution of specimen electrode interface to the total observed resistance of the sample electrode assembly.

For the sample with $x = 0.01$, an arc passing through the origin in the high frequency range and another in

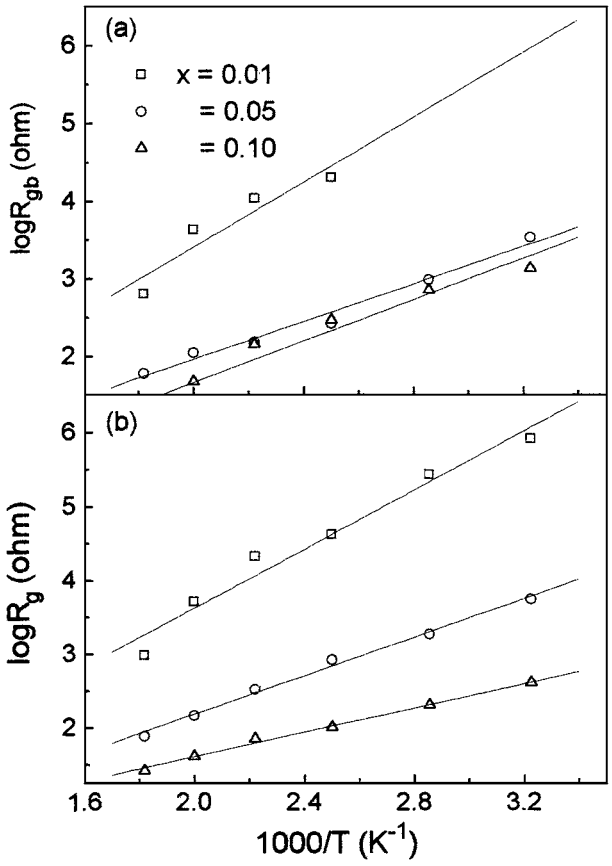

Figure 7 Variation of (a) log R_g and (b) log R_{gb} with 1000/T for various compositions in the system $BaSn_{1-x}Co_xO_3$.

the intermediate frequency range represent the contribution of the grains and grainboundaries respectively. Electrode polarization contribution appears only at high temperature. For $x = 0.05$ and 0.10, the contribution of the bulk is given by the intercept of the high frequency arc on the Z' axis on the origin side. Values of resistance for contribution of grains R_g, grainboundaries R_{gb} and electrode specimen interface R_{el} to the total observed resistance were obtained from the intercept of the arcs on the Z' axis at a few selected temperatures for different compositions from their respective complex plane impedance plots. Plots of log R_g and log R_{gb} vs 1000/T for different compositions are shown in Fig. 7. It is to be noted that both the grains and grainboundaries resistance decrease with increasing concentration of cobalt ions i.e. increasing x. Resistance contribution for sample electrode interface is small for all the samples. For the sample with $x = 0.01$ containing small concentration of cobalt ions, the grain resistance R_g is higher than the grainboundaries resistance R_{gb} whereas for the samples with $x = 0.05$ and 0.10 containing higher concentration of cobalt ions, the grain resistance R_g is very much smaller than that of grain boundaries R_{gb}. Plots of log R_g and R_{gb} vs 1000/T can be fitted to a straight line. The values of activation energy of conduction for the grains and grainboundaries determined by least square fitting of the experimental data are given in Table II. It is to be noted from the Table II that the values of activation energies E_g and E_{gb} for the sample with $x = 0.01$ are higher than the corresponding values for the samples with $x = 0.05$ and 0.10. It is interesting to note that the values of activation energy for conduction obtained from the log σ_{dc} vs 1000/T plots (Fig. 4) are close to the values of E_{gb} for the various samples. This shows that the conductivity behaviour in these materials is dominated by grainboundaries. This is expected as grainboundaries form the continuous phase.

$BaSnO_3$ is a wide band gap material having an energy gap 3.4 eV ssimilar to SnO_2 in which valence band consisting of oxygen 2p "lone pair" orbital is separated from the conduction band of Sn, s orbitals by 3.6 eV [10, 11]. The observed values of activation energies of conduction (Table II) rule out the possibility of any intrinsic conduction observed in the temperature range of measurements. The resistivity decreases with increase in concentration of cobalt ions. This shows that conduction in these materials is dominated by cobalt ions.

Majority of the cobalt ions are in +3 state in these materials and act as acceptors on Sn^{4+} sites. These acceptors ionize giving rise to holes in the valence band which act as majority charge carriers. Both electrons as well as holes contribute to the conduction in these materials, as explained below, the holes being majority charge carriers. This is in conformity with p-type conductivity (+ve value of α). Variation of Seebeck coefficient, α with temperature in these materials is similar to that observed in the $M_{1-x}La_xTi_xCo_{1-x}O_3$ (M = Ca, Sr and Ba) systems [12–14]. Initially α increases with temperature slightly and then remains constant. Initial increase in α is due to ionization of traces of donor Co^{2+} ions generating electrons. When all the donor states are ionized, α becomes constant with temperature. This has been explained in terms of loss of oxygen occurring in these materials in traces at high temperature during their sintering in accordance with the reaction.

$$O_O \Leftrightarrow \frac{1}{2}O_2 + V_0^{\bullet\bullet} + 2e' \qquad (2)$$

where all the species are written in accordance with Kröger-Vink notation of defects. The electrons released in the above process may be captured by Co^{3+} ions to generate Co^{2+} ions. These Co^{2+} ions act as donor (have an additional electron as compared to Co^{3+} ions). With increase in temperature, they give this electron to the conduction band.

Constant value of α at high temperature shows that number of charge carriers remains constant. Increasing value of conductivity with increasing temperature, therefore, shows that mobility is thermally activated. The value of Seebeck coefficient is high and it is almost independent of temperature above a particular temperature. Further value of α as well as activation energy of conduction decreases with increasing concentration of cobalt ions. All these feature indicate that conduction occurs due to hopping of charge carriers among localized sites associated with cobalt ions as small polarons. i.e. among Co^{2+} and Co^{3+} sites. Similar behavior is observed in the system $La_{1-x}Sr_xCrO_3$ [15].

4. Conclusions

Solid solution forms for all the compositions studied in the $BaSn_{1-x}Co_xO_3$ system. All the compositions have cubic structure. They exhibit p-type conduction showing conduction is dominated by cobalt ions. From temperature dependence of Seebeck coefficient and conductivity, it is concluded that mobility is thermally activated and conduction occurs due to hopping of charge carriers among localized sites associated with cobalt ions.

Acknowledgements

One of the author (K. K. Srivastav) is grateful to UGC for providing Research Associateship during the course of this work. We are grateful to Prof. Dhananjai Pandey, Coordinator of School of Materials Science & Technology, IT - BHU for providing XRD facility. We are also thankful to Department of Science and Technology, New Delhi for financial assistance.

References

1. B. JAFFE, W. R. COOK JR. and H. JAFFE, in "Piezoelectric Ceramics" (Academic Press, New York, 1971) p. 121.
2. R. C. BUCHANAN, in "Ceramic Materials for Electronics" (Marcel Decker, New York, 1986) p. 69.
3. Y. SHIMIZU, M. SHIMABUKURO, H. ARAI and T. SEIYAMA, *J. Electrochem. Soc.* **136** (1989) 1206.
4. U. LAMPE, J. GERBLINGER and H. MEIXNER, *Sensors and Actuators B, Chem* **26/27** (1995) 97.
5. *Idem.*, *ibid.* **24/25** (1995) 657.
6. H. S. TEWARI, Ph.D. thesis, Banaras Hindu University, India, 1994.
7. S. UPADHYAY, Ph.D. thesis, Banaras Hindu University, India, 1998.
8. I. M. HODGE, M. D. INGRAM and A. R. WEST, *J. Electroanal. Chem.* **74** (1976) 125.
9. H. S. MAITI and R. N. BASU, *Mat. Res. Bull.* **21** (1987) 1107.
10. R. J. CAVA, P. GAMMEL, B. BATLOGG, J. J. KRAJEWSKI, W. F. PECK JR., L. W. RUPP JR., R. FELDER JR. and R. B. V. DOVER, *Phys. Rev. B* **42** (1990) 4815.
11. S. MUNNIX and M. SCHMEITS, *ibid.* **27** (1983) 7624.
12. D. KUMAR, CH. D. PRASAD and O. PARKASH, *J. Phys. Chem. Solids* **51** (1990) 73.
13. O. PARKASH, CH. D. PRASAD and D. KUMAR, *J. Phys. D: Appl. Phys.* **27** (1994) 1509.
14. D. KUMAR, CH. D. PRASAD, H. S. TEWARI and O. PARKASH, *J. Phys. D: App. Phys.* **23** (1990) 342.
15. D. P. KARIM and A. T. ALDRED, *Phys. Rev. B* **20** (1979) 2255.

Received 1 November 2000
and accepted 14 August 2001